

REAR-IMPACT INFLICTED TEMPOROMANDIBULAR JOINT INJURY

C.G.Lyons, C.K.Simms & C.L.Brady,

Department of Mechanical & Manufacturing Engineering

Trinity College Dublin. Ireland

e-mail clyons@tcd.ie

Journal of Crash Prevention and Injury Control, vol 2(4) pp257-269, 2000

ABSTRACT

Indirect injuries to the jaw can lead to a range of painful symptoms with serious consequences. These injuries are confirmed by clinical evidence but the injury mechanism is not understood. This work is an investigation into the nature of the injury process.

We have previously reported on the impact testing of a mechanistic model of a human head, neck and mandible. Results showed high angular velocities and accelerations of the mandible, but the magnitude of mouth opening lay within physiological limits. This paper reports on further impact tests using the same physical model to determine the kinematic behaviour of the temporomandibular joint (TMJ) during whiplash. In addition, human cadaveric samples were tested to quantify some structural properties of the TMJ. The results from this and data from a mathematical model of the TMJ are reported.

key words; TMJ, mandible, human-surrogate, injury, rear-impact, MVA's

INTRODUCTION

The TMJ is a synovial hinge joint formed between the condyle of the mandible and the glenoid fossa on the squamous part of the temporal bone. A fibro-cartilaginous disc lies between these two bony elements, permitting easy movement between mandible and

cranium. The TMJ is capable of a range of motions both gross and subtle and is under the control and restraint of the masseter, lateral & medial pterygoid, the temporalis and other muscles, and the temporomandibular ligament. The joint capsule consists of a thin sheet of collagen bound down to the neck of the condyle inferiorly, and to the rim of the glenoid fossa superiorly, Figure.1. The superior belly of the lateral pterygoid muscle inserts into the antero-medial portion of the TMJ meniscus. The inferior belly of the same muscle has attachments onto the neck of the condyle. Mouth opening consists of a combination of rotation and translation of the condyles over the articular eminence. The joint is therefore complex and comprised of elements that may be, singularly or in combination, subject to trauma.

There have been many reports of damage to the TMJ, but most fail to present solid evidence of the aetiology of the injury. Typical of them is the work of Garcia and Arrington [1996] who report on MRI investigations of eighty-seven consecutive MVA whiplash patients presenting with TMJ dysfunction symptoms. According to self-reports, none had suffered a direct trauma to the head, neck, or mandible and none had symptoms prior to their accident. The MRI tests were evaluated for disc displacement, reduction, effusion and inflammation/oedema. The authors report internal derangement in eighty-seven percent of cases based on T1 weighted images. Abnormal joint fluid was seen in T2 weighted samples.

The difficulty with this clinical evidence is that no two reports are sufficiently similar in structure to allow cross-comparison. In addition, some critical questions do not seem to have been asked. With the exception of Magnusson [1994], none of the surveyors attempted to differentiate between injuries caused by direct and indirect trauma. The percentage of a sample involved in litigation is important in assessing the reliability of self-reports, yet this is not documented in several studies. Neither is the small sample size of most surveys adequately addressed. There are a disproportionate number of females in almost all samples, but it has also been noted that females are more prone to seeking healthcare in general.

Recently, McKay & Christensen [1998] contended that the reputed symptoms of whiplash injuries are in fact due to progressive synovitis, osteoarthritis and internal derangement that evolve throughout adult life in 25-35% of the population. It is certainly true that other

disorders share some or all of the same signs and symptoms as those claimed by victims of mandibular whiplash, thereby casting further doubt on the reliability of these epidemiological reports.

A slight majority of surveys favour a causal link, but the clinical evidence is inconclusive - neither the proponents nor the opponents of 'jawlash' have provided conclusive proof. There are too many factors involved; patient selection methods, predisposition to injury, litigation, type of patient likely to attend a given clinic, posture and state of preparedness (a head turned at the time of impact greatly reduces the range of neck motion, Schneider *et al.* [1975].) In one study, sixty-eight percent of TMJ patients also suffered from nervous stomach disorders, Molin [1973]. These clinical surveys show that there are a considerable number of patients with dysfunction of the TMJ and although there is no evidence that conclusively links whiplash to TMJ dysfunction, it has not been possible to demonstrate adequately that there is no causal link.

Injury Mechanisms There are two main proposed injury mechanisms: either injury occurs due to inertial behaviour of the mandible during whiplash, or neurological changes in the post accident period cause muscle spasm and, with time, internal derangement of the TMJ. These two postulates are called the Inertial Injury Theory (IIT) and Late TMJ Injury Theory (LTIT) respectively. The proponents of the IIT claim that excessive mouth opening occurs because the lower jaw does not keep up with head motion, Mannheimer *et al.* [1989], Pullinger & Seligmann [1991], Roydhouse [1973], Weinberg & Lapointe [1987]. Further, it is proposed that hypertranslation of the condyles occurs easily due to the weakness/absence of the anterior capsule, Mahan [1980], Weinberg & Lapointe [1987].

The mechanism proposed by the LTIT is very different. Voluntary control of body posture and movement is governed by the musculature via neural impulses. However, if posture is altered by injury, misinterpretation by the proprioceptors could produce ongoing neurological signalling, resulting in pathofunction of the related structures. The LTIT indicates that pathofunction in the cervical musculature is an important aetiological factor in the development of TMJ or facial pain, Lader [1983].

The IIT is quoted as the primary cause of TMJ dysfunction. It has two major flaws: if injury is caused during the accident, why is the onset of symptoms often delayed? Secondly, do the proposed rearward motions of the head and mandible actually occur? In contrast, the LTIT is supported by the late onset of symptoms, but the theory cannot be experimentally validated. However, if whiplash related TMJ injuries do exist, but loading at the TMJ during the whiplash sequence is benign, then this constitutes strong evidence in favour of the LTIT.

IMPACT TESTING

We have previously reported, Lyons *et al.* [1997], on the construction and testing of a mechanistic model of the human head, neck and mandible. This model was validated by comparison with the retroflexion data from the human volunteer tests of McConnell *et al.* [1995]. Tests showed that for purely passive and for 25% active muscles, mouth opening was a feature of the retroflexion phase of whiplash. In particular, for a Δv of 9.2km/h and purely passive (relaxed) elevator muscles, a maximum mouth-opening angle of *ca.* 20 degrees was measured, see Figure 2. Sled tests with the 25% muscles in place showed that the increased muscle force diminished mouth opening to *ca.* 2 degrees and from this it was concluded that testing with the 50% and 100% active muscles was unnecessary.

EXPERIMENTAL TESTS: KINEMATICS OF THE TMJ

The kinematic behaviour of the TMJ was investigated in a further experimental series. The TMJ is fixed in the skull and experiences forces corresponding to the kinematic behaviour of the head and jaw. It was not practical to attach a biaxial accelerometer to the mandible at the TMJ, and direct measurement of loads across the articular surfaces could therefore not be realised. However, examination of the accelerations at the skull portion of the TMJ allowed a more limited analysis. It should be clear that these measurements alone cannot be used to calculate subsequent TMJ loading. An estimate of the latter will be made using the results of a numerical simulation. At this stage, experimental measurements of (skull portion) TMJ

kinematics are used to show that proximity to the centre of gravity (cog) of the head protects the TMJ from large linear accelerations.

TMJ Accelerations A pair of orthogonal linear accelerometers were fixed at the TMJ in the sagittal plane, Figure 3. Coupled with an accurate measurement of head angular displacement (θ_{head}), Lyons *et al.* [1997], these were used to calculate (X , Z) direction accelerations directly, see Figure 4. The maximum resultant magnitude in the sagittal plane does not exceed 30ms^{-2} . The X component is positive throughout retroflexion, but it can be seen that the magnitude of these compressive accelerations is small ($<1\text{g}$) and fluctuating during the early stages of retroflexion.

TMJ displacement The instantaneous centre of rotation (ICR) is the only point of a moving lamina in planar motion (not in pure translation) with zero velocity, and any point on the body experiences forces proportional to its distance from the ICR. The human skull does not have a unique pivot point: its ICR is therefore not fixed and its locus is important during the whiplash sequence. The ICR was computed from the displacements of two points on the head. These were determined using the following measurements, (1) absolute X - displacement of the sled (P_{sledX}), (2) relative X & Z - displacements ($P_{headX/sledX}$ & $P_{headZ/sledZ}$) between head centre of gravity (cog) and the sled ($P_{headX/sledX}$) and (3) angular displacement of the head (θ_{head}).

An arrangement of optical-switches and graticules was used to measure P_{sledX} and $P_{headX/sledX}$ and linear and rotational potentiometers were used for $P_{headZ/sledZ}$ and θ_{head} respectively. The absolute X displacement of the head cog is the algebraic sum of P_{sledX} and $P_{headX/sledX}$, and $P_{headZ/sledZ}$ is equivalent to absolute Z displacement of the head. Time histories of the head cog displacement in the sagittal plane could thus be established and θ_{head} can then be used to calculate the corresponding displacement of the TMJ. In the upright pre-impact position, the polar coordinates of the TMJ relative to the head cog are $r_I = x_I^2 + z_I^2$ and $\theta_I = \tan^{-1}(z_I/x_I)$, where $x_I = 0.01\text{m}$ and $z_I = 0.02\text{m}$, see Figure 5. As the head rotates,

$$P_{TMJ_x} = P_{head_x} + r_1 \cos(\theta_1 - \theta_{head}) \dots\dots\dots(1)$$

$$P_{TMJ_z} = P_{head_z} - r_1 \sin(\theta_1 - \theta_{head}) \dots\dots\dots (2)$$

The X , Z coordinates of two points on the head are then known and the ICR can be calculated.

After impact, X direction motion of the sled occurs, Figure 6a. The inertia of the head causes its response to lag behind sled motion and the head cog therefore moves rearwards relative to the sled. The sled and head are both at rest prior to the impact, and inertial loading of the TMJ is a function of its kinematic behaviour relative to a fixed reference frame and not a frame fixed in the sled. Absolute X direction displacement of the head cog is equal to the sum of sled displacement and head cog displacement relative to the sled. A considerable degree of cancellation occurs: as the sled travels forward, relative motion of the head is rearward. From Figure 6b it is clear that P_{head_x} is small throughout the retroflexion sequence of the head.

TMJ displacements differ from head cog displacements only due to head rotation. Motion of the TMJ in the X direction occurs gradually during the retroflexion sequence and this accounts for the low acceleration levels measured at the TMJ, see Figure 4. These results are unsurprising: the head is the dominant mass and consequently minimises its linear and angular velocities. The TMJ lies close to the head cog and experiences correspondingly small displacements.

Head ICR During retroflexion, the locus migrates from a postero-superior location to close to the TMJ and then to an antero-superior location, Figure 7a. During the greater part of the retroflexion period, the head ICR lies close to the TMJ, see Figure 8. Initially, when $\dot{\theta}_{head}$ is small, the ICR lies far from the TMJ. As $\dot{\theta}_{head}$ increases, the ICR is rapidly pulled in closer to the TMJ. Then, as $\dot{\theta}_{head}$ decreases again to zero at maximum retroflexion ($t = 0.18s$), the locus of ICR once again migrates away from the TMJ. The calculated locus is highly sensitive to instrumentation error and the greatest ambiguity occurs when $\dot{\theta}_{head}$ is small. By

definition, the ICR lies at infinity when $\dot{\theta}_{head} = 0$. The resolution of the P_{sledX} and $P_{head/sledX}$ measurements were limited to $\pm 0.001m$ and this was sufficient to cause considerable error in the locus of the ICR during the initial and final stages of retroflexion. Thus there is some conflict between the accelerometer data and the computed locus of ICR head between $t=0$ and $t=0.03s$. The accelerometer measurements are positive throughout retroflexion, see Figure 4. In contrast, the ICR measurements indicate an initial tensile load as the ICR lies to the left of the TMJ and initial head rotation is anticlockwise, see Figure 7. The measured TMJ accelerations at the onset of retroflexion are small and fluctuating, while the ICR measurements are unreliable because $\dot{\theta}_{head}$ is still small. The result is that the two measurements err either side of zero.

MATHEMATICAL MODELS

Free Body Diagram It is accepted that the mammalian TMJ is load bearing during functional movements, Barbenel [1972], Hylander [1979], Brehnan *et al.* [1981]. The design of the human TMJ is ideal for load distribution across the articular surfaces, Osborn [1985], but experimental verification has proved difficult. Brehnan *et al* measured low level loading (ca. 13N) during molar chewing in macaque TMJ's while Hylander measured bone strain in the condylar neck and found qualitative evidence of a compressive reaction force during the power stroke of mastication, but failed to quantify the load.

A sagittal plane free body diagram (FBD) of the mandible indicates considerable loading of the articular surfaces during functional biting, see Figure 8. The principal bite-force generators and the corresponding reaction forces have been approximated as point loads. These are: occlusal or bite force (F_b) acting at an angle ϕ to the vertical, muscle force (F_m) at an angle θ to the vertical and the orthogonal components of TMJ reaction force. The line of action of tensile load in the temporomandibular ligament is also shown. There is no load on this ligament during bilateral biting. Taking moments about the TMJ gives:

$$F_b r_b - F_m r_m = 0 \dots\dots\dots(3)$$

Clockwise moments are positive and r_b and r_m are the moment arms of F_b and F_m about the TMJ. The joint reaction forces have no moment about the TMJ. The magnitude of the bite force is less than the applied muscle force by a factor of $r_b/r_m \cos(\theta - \phi)$

A vertical force balance gives:

$$F_m \cos \theta - F_b \cos \phi - F_{j_z} = 0 \dots\dots\dots(4)$$

Since $F_m \cos \theta > F_b \cos \phi$, there must be a vertical compressive reaction force in the TMJ. Van Eijden *et al.* [1990] investigated muscle activation for various pre-defined bite forces measured at the second pre-molars and registered a maximum bite force of ca. 600N. If this is applied and the angles θ , $\phi = 0$ and $r_b = 1.5r_m$, then by equations 3 and 4 the vertical reaction force at the TMJ ≈ 300 N. The horizontal reaction is smaller:

$$F_m \sin \theta - F_b \sin \phi - F_{j_x} = 0 \dots\dots\dots(7)$$

The angles θ and ϕ will be small in most functional positions. The mechanical disadvantage of the muscle force dictates (as before) that $F_m \sin \theta > F_b \sin \phi$ and the horizontal joint reaction force required for force balance is therefore compressive.

This FBD is a major simplification: the actions of the digastric muscle and the lateral pterygoid have been omitted. Further, the direction of the force vectors generated by each muscle depends on the recruitment levels of their individual fibres. However, this analysis does show that considerable vertical loading at the TMJ occurs during functional biting.

Kinematic model The experimental work can be used to construct a kinematic model of jaw behaviour during retroflexion. Jaw kinematics are determined by its inertial characteristics, head movement and the biomechanical constraints linking the mandible to the skull. The experimental evidence is used to calculate values for the model parameters: if the simulations show good correlation between the model and dummy, then a parametric analysis using the model can be used to investigate the stability of the dummy. However, strict simplifications are necessary to allow the governing differential equations of the system to be derived.

Schneider *et al.* [1989] have previously modelled the dynamics of the head, neck and mandible, predicting very large angles of mouth-opening (1.17rad and 1.11rad) for simulated impact speeds of 6.71ms^{-1} and 13.41ms^{-1} respectively. Translation of the condyles was also reported. However, the constraints provided by the muscles and ligaments were not modelled and jaw motion was therefore governed purely by inertial characteristics. The low inertia of the mandible and high strength of the elevator muscles strongly compromises the validity of these simplifications and the predicted results are therefore questionable.

Experimental measurements of head kinematics were used as input to a Lagrangian model, see Figure 9. The head is a rigid body rotating through an angle θ about a fixed point I . The TMJ lies at a radius r from I . The mandible is also a rigid body (centre of mass M , distance c from the TMJ). The mandible has three degrees of freedom (DOF) in the sagittal plane: linear displacements (x_1 & x_2) resisted by linear springs (k_1 and k_2) and rotation through an angle ϕ , resisted by a rotational stiffness k_3 . Damping is not included as maximum displacements were desired.

Energy functions Application of Lagrange's method yields three equations of motion:

$$Lx_1 = M \ddot{x}_1 + Mx_2 \ddot{\theta} + 2M \dot{x}_2 \dot{\theta} + Mc(\dot{\theta} - \dot{\phi}) \sin \phi + Mc(\ddot{\theta} - \ddot{\phi}') \sin \phi + 2Mc \dot{\theta} \dot{\phi} \cos \phi - Mc(\dot{\theta}^2 + \dot{\phi}^2) \cos \phi - M(r + x_1)\dot{\theta}^2 + k_1x_1 = 0$$

$$Lx_2 = M \ddot{x}_2 - M(r + x_1)\ddot{\theta} + 2M \dot{x}_1 \dot{\theta} + 2Mc \dot{\theta} \dot{\phi} \sin \phi + Mc(\ddot{\theta} - \ddot{\phi}) \cos \phi + 2Mc \dot{\theta} \dot{\phi} \cos \phi - Mc(\dot{\theta}^2 + \dot{\phi}^2) \sin \phi - Mx_2\dot{\theta}^2 + k_2x_2 = 0$$

$$L\phi = \frac{4}{3}Mc^2 \ddot{\phi} - Mc\ddot{\theta} - 2Mc \dot{x}_1 \dot{\theta} \cos \phi - Mc(r + x_1)\ddot{\theta} \cos \phi + Mc \ddot{x}_2 \cos \phi + Mc(r + x_1)\dot{\theta}^2 \sin \phi - Mc(\dot{x}_1 + x_2 \dot{\theta} + 2 \dot{x}_2 \dot{\theta}) \sin \phi - Mcx_2\dot{\theta}^2 \cos \phi + k_3\phi = 0$$

These may be expressed in the form $[A]\{\ddot{q}_i\} = [B]$, where

$$A = \begin{bmatrix} M & 0 & -Mc \sin \phi \\ 0 & M & Mc \cos \phi \\ -Mc \sin \phi & Mc \cos \phi & \frac{4}{3}Mc^2 \end{bmatrix}$$

The determinant of [A] is non-zero for all non-trivial cases and numerical integration was used to solve this system of equations.

Parameter values The choice of values for spring coefficients, link lengths and head kinematics resulted from previous experimental work. Parameters k_1 and k_2 represent internal stiffness of the TMJ and k_3 is the rotational stiffness representing the moment of the passive elevator muscles. Values for these parameters were estimated from cadaveric tissue tests, Simms [1999], synthesised in Table I. The values for head kinematics were interpolated at each integration time step from the experimental sled tests at 9.2km/h Δv .

Results The strongly oscillating curves reflect the absence of damping in the system, Figure 10a & b. It can be seen that x_1 and x_2 are small, but ϕ rises steadily to a maximum of 0.43rad between $t=0.1s$ and $t=0.17s$, Figure 10c. Considerable mouth opening occurs but displacements within the TMJ are small.

The angle ϕ represents mouth opening and there is quite good correlation between the degree of mouth opening on the mechanical dummy and ϕ predicted by the numerical model, see Figure 10c. The predicted level of mouth opening is higher than the experimental result because no damping has been included in the mathematical model. After the mouth has closed, the comparison between the two curves loses validity as the mathematical model does not accommodate the effects of occlusal contact. In addition, the angle of mouth opening on the physical model is derived from numerical integration, which becomes very poor after occlusal impact.

Estimation of TMJ Reaction forces An estimate of the orthogonal forces developed within the TMJ can be found from the respective products, $k_1 x_1$ and $k_2 x_2$, see Figure 10a & b. The linear stiffness of both k_1 and k_2 is 5000N/m. The maximum loads generated by the

whiplash sequence for a Δv equivalent of 9.2km/h are therefore 10N and 6.2N in the x_1 and x_2 directions respectively. Positive forces are tensile.

A parametric analysis showed that in all of the simulations the predicted forces were far less than those generated in functional biting. These predictions indicate that inertial load developed at the TMJ during whiplash is of a much lower magnitude than the reaction forces during functional movements.

CADAVERIC SPECIMEN TESTING

The mechanical properties of the soft tissues of the TMJ are poorly documented and the variable collagen content, fibre orientation and geometry preclude adaptation of data from tests on other ligamentous materials. Formalin preserved cadaveric specimens consisting of a section of the skull including the intact TMJ and a section of the mandible were used to experimentally determine some of the structural properties of the joint. The bony sections of both skull and mandible were fixed in acrylic blocks and the mandibular aspect was affixed to a "slider" system, allowing the condyle to "glide" over the eminence of the fossa as it would *in vivo*.

The Force - Elongation curve shows the quasi-static behaviour of three such samples, see Figure 11. There is quite close agreement within each sample but a high variability between samples. This is a consequence of considerable geometric variations between different TMJs, even in the two sides of the same subject, McDevitt [1989]. Post-test inspection of the samples showed no exterior signs of injury, and a healthy *in-vivo* subject can easily achieve a protrusion of 5mm.

During mouth opening, the mandible both rotates and translates. This motion cannot be reproduced in a tensile testing machine and the force required to protrude/distract the mandible for various fixed angles of mouth opening (0, 5 and 10 degrees) was measured instead, Figure 12. The effect of mouth opening is to increase stiffness at low displacements and decrease it at higher displacements, but it is clear that the magnitude of the load is not greatly altered.

The strain rate dependency of TMJ stiffness was also investigated. This dependency is a consequence of the visco-elastic behaviour of biological tissue, where the load produced by stretching depends also on the rate of stretch. A number of empirical laws have been developed to predict the probability of injury for a given strain rate. The viscous criterion (VC), Lau and Viano [1986], predicts that the critical velocity for strain-rate dependent injuries is 3ms^{-1} and that below this level visco-elastic effects are not critical. Retroflexion in whiplash occurs over *ca.* 130ms: 5mm stretch in 130ms is a stretch velocity of 0.38m.s^{-1} . This is far below the threshold level, but it is possible that the VC is not a suitable predictor for soft tissue trauma to the TMJ.

A dynamic materials testing analyser (Rheometer Ltd. DMTA Mk3) was used to assess damping within the TMJ over a range of frequencies (0-30Hz). Retroflexion of the head in 130ms is a close approximation to a quarter sine wave, corresponding to *ca.* 2Hz. Strips of ligamentous material dissected from the capsule of a human TMJ were clamped in the DMTA and a predefined cyclic strain was applied. The resulting elastic modulus (ratio of stress to strain) and $\tan(\delta)$ (ratio of viscous/elastic moduli) are shown in Figure 13a & b. The viscous modulus was calculated from the following equations.

$$\text{Elastic Modulus: } E' = \cos\delta(\sigma/\epsilon). \quad \text{Viscous Modulus: } E'' = \sin\delta(\sigma/\epsilon)$$

$$\text{Complex Modulus: } E^* = \sqrt{(E')^2 + (E'')^2} \quad \text{Phase Angle: } \tan\delta = (E''/E')$$

Results from these tests showed large experimental scatter: the elastic modulus varied between 2MPa and 6MPa and showed no recognisable trend over the frequency range of 0-30 Hz. The elastic modulus from the quasi-static force-extension tests was calculated by estimating the cross-sectional area of joint tissue as 15mm^2 . The force at 5mm stretch varied between 13N and 35N, see Figure 11, and the corresponding stress is 0.86-2.3MPa. Strain in the tissue fibres was estimated by assuming that 5mm extension represents *ca.* 30% strain. The resulting elastic modulus is 2.8-7MPa, and there is therefore good agreement between the two modes of testing. The DMTA tests showed that the maximum viscous contribution to the overall modulus in the frequency range tested was 20%. The implication is that although some strain dependent resistance to loading develops, the extent of this is not critical.

CONCLUSIONS

The results indicate that the mandible and TMJ are not harmed during a low velocity rear end collision. Excessive levels of mouth opening do not occur from Δv 's up to 9.2km/h. Linear accelerations at the skull portion of the TMJ measured during sled tests are low due to the protection provided by the proximity of the TMJ to the head centre of gravity. Investigation of head kinematics showed that linear motion of the head centre of gravity was small throughout the retroflexion phase.

An order of magnitude analysis between TMJ reaction forces during functional biting and inertial loading during retroflexion shows that the former produces much higher loading. Soft tissue tests of in vitro specimens have been used to quantify some of the structural properties of the TMJ. The effects of mouth-opening and viscoelasticity are significant but not sufficient to cause injury during whiplash. The data from these soft tissue tests and from the sled tests was used to develop a 2-D Lagrangian model. Simulated levels of mouth opening compared well to sled tests, and a parametric analysis showed that even significant variations are unlikely to affect loading at the TMJ during whiplash.

Soft tissue tensile tests using embalmed cadaveric specimens indicated that considerable loads are required to cause anterior dislocation of the condyles. The effects of mouth opening and visco-elasticity were investigated: neither proved sufficient to damage the joint. At the Δv 's used, our results preclude trauma explained by hyperextension injury. Temporomandibular joint dysfunction is more likely due to post accident neuro-muscular changes and/or pain referral of a cervicogenic nature.

The Late TMJ Injury Theory (LTIT) proposes that post accident neurological changes cause radiated pain to the TMJ. It has been noted that this theory cannot be experimentally validated. However, none of the findings reported in this paper contradict this theory. The literature review shows there is some connection between TMJ and whiplash. It is unlikely that injuries occur during the whiplash event: it is therefore concluded that TMJ injuries arising from whiplash develop in the post accident period. This adequately explains the frequent delay in the onset of symptoms.

The implication is that an investigation of crash kinematics is not a suitable means of

assessing the likelihood of TMJ disorders following whiplash. Instead, an assessment of the extent of neuromuscular changes emanating from the neck region is probably a better indicator of TMJ disorders following whiplash.

ACKNOWLEDGEMENTS

To Prof. M O'Brien, Head of the Dept of Anatomy, Trinity College Dublin, for helpful discussion and for the use of facilities and to Prof. W McDevitt for permission to use Figure 1.

REFERENCES

Barbenel, J. C. (1972) The Biomechanics of the Temporomandibular Joint, *J Biomechanics*, Vol 5. pp. 251-256.

Brehnan, K., Boyd, R. L., Laskin, J., Gibbs, C. H. & Mahan, P. (1981) Direct measurement of loads in the temporomandibular joint in macaca arctoides, *J Dent Res*, Vol. 60, pp.1820-1824.

Garcia, R. Jr. & Arrington, J. A. (1996) The Relationship Between Cervical Whiplash and Temporomandibular Joint Injuries: an MRI Study, *J Craniomandibular Practice*, Vol. 14, pp. 233-239.

Hylander, W. (1979) An Experimental Analysis of Temporomandibular Reaction Force in Macaques. *Am J Phys Anthropol*, Vol. 51, pp. 433-456.

Lader, E. (1983) Cervical Trauma as a Factor in the Development of TMJ Dysfunction and Facial Pain, *J Craniomandibular Pract.*, Vol. 1, pp. 87-90.

Lau, V. & Viano, D. (1986) The Viscous Criterion - Bases and Applications of an Injury Severity Index for Soft Tissues, *30th Stapp Car Crash Conference, SAE Trans* Vol. 95, pp. 123-141.

Lyons, C.G., Brady, C.L. & Simms, C. (1997) An Investigation of Damage to the Human Temporomandibular Joint, *Proc of 41st Annual AAAM*, pp. 315-330.

McConnell, W.E., Howard, R.P., vanPoppel, J., Krause, R., Guzman, H., Bomar, J., Radin, J., Benedict, J. & Hatsell, C. (1995) Human Head and Neck Kinematics after Low Velocity Rear-End Impacts- Understanding "Whiplash", *SAE Trans.* Vol. 104, Sec. 6, pp. 215-238.

McDevitt, W. E. (1989) *Functional Anatomy of the Masticatory System*. Butterworth and Co.

McKay, D. C. & Christensen, L.V. (1998) Whiplash Injuries of the Temporomandibular Joint in Motor Vehicle Accidents: Speculation & Facts, *J Oral Rehabilitation* Vol. 2, pp. 731-746.

Magnusson, T. (1994) Extra-cervical Symptoms after Whiplash Trauma, *Cephalgia*. Vol. 14, pp. 223-227

Mahan P. E., (1980) *The Temporomandibular Joint in Function and Pathofunction*, Quintessence Publishing Co.

Mannheimer, J., Attanasio, R., Cinotti, W. & Pertes, R. (1989) Cervical Strain and Mandibular Whiplash: effects upon the Craniomandibular Apparatus, *Clinical Preventive Dentistry*, Vol. 11, pp. 29-32.

Molin, C. (1973) Studies in Mandibular Pain Dysfunction Syndrome, *Swed. Dent. J.* Vol. 66, No.1, (supplement No 4)

Osborn, J.W. & Baragar, F.A. (1985) Predicted Pattern of Human Muscle Activity During Clenching Derived From a Computer Assisted Model: Symmetric Vertical Bite Forces, *J.Biomechanics*. Vol. 18, pp. 599-612.

Pullinger, A. G. & Seligman, D. A. (1991) Trauma History in Diagnostic Groups of Temporomandibular Disorders, *J Oral Surg*, Vol. 71, pp. 521-534.

Roydhouse, R. H. (1973) Whiplash and Temporomandibular Dysfunction, *The Lancet*, pp.1341-1342.

Schneider, L.W., Foust, D.R., Bowman, B.M., Snyder, R.G., Chafin, D.B., Abdelnour, T.A. & Baum, J.K. F. (1975) Biomechanical Properties of the Human neck in Lateral Flexion, *19th Stapp Car Crash Conference*. Warrendale PA. pp. 455-485.

Schneider, K., Zernicke, R.F. & Clark, G. (1989) Modeling of Jaw-Head-Neck Dynamics During Whiplash, *J Dent Res*, Vol. 68, pp.1360-1365.

Svennson, M.Y. & Loevsund, A. (1992) A Dummy for Rear End Collisions- Development and Validation of a New Dummy Neck, *Proc 1992 Intl IRCOBI Conf*, Verona, Italy, pp. 299-310.

Szabo, T.J. & Welcher, J.B. (1996) Human Subject Kinematics and Electromyographic Activity During Low Speed Rear Impacts, *Society of Automotive Engineers, SAE Transactions*, No. 96, pp. 24-32.

Weinberg, S. & Lapointe, H. L., (1987) Cervical Extension-Flexion injury (Whiplash) and Internal Derangement of the Temporomandibular Joint, *J Oral Maxillofacial Surg*, Vol. 45, pp. 653-656.

Yamada, H. (1970) *Strength of Biological Materials*, Williams and Wilkins Co., Baltimore. MD.

TABLES:

Parameter	<i>M</i>	<i>R</i>	<i>c</i>	<i>k₁</i>	<i>k₂</i>	<i>k₃</i>
Value	0.2kg	0.04m	0.05m	5000N/m	5000n/m	0.78Nm/rad

Table I. Parameter Values of the Lagrangian Model

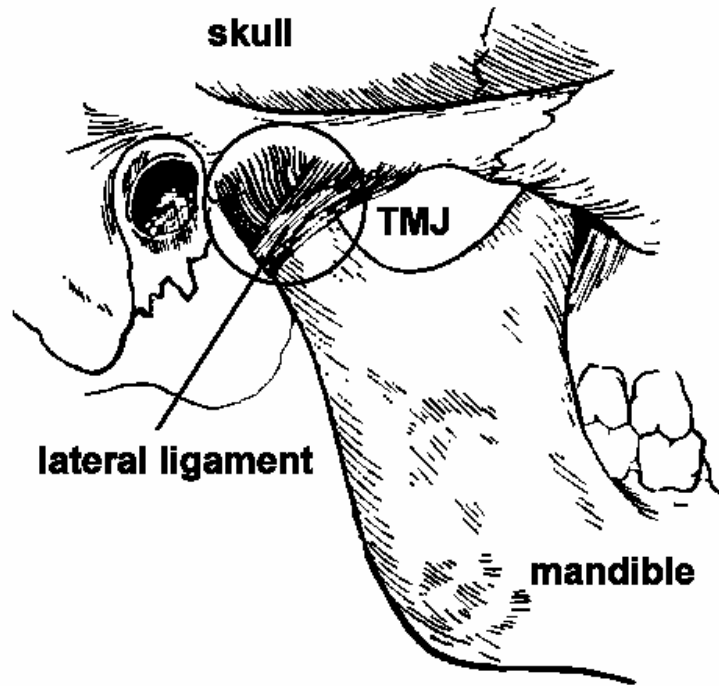


Figure 1. Lyons et al.

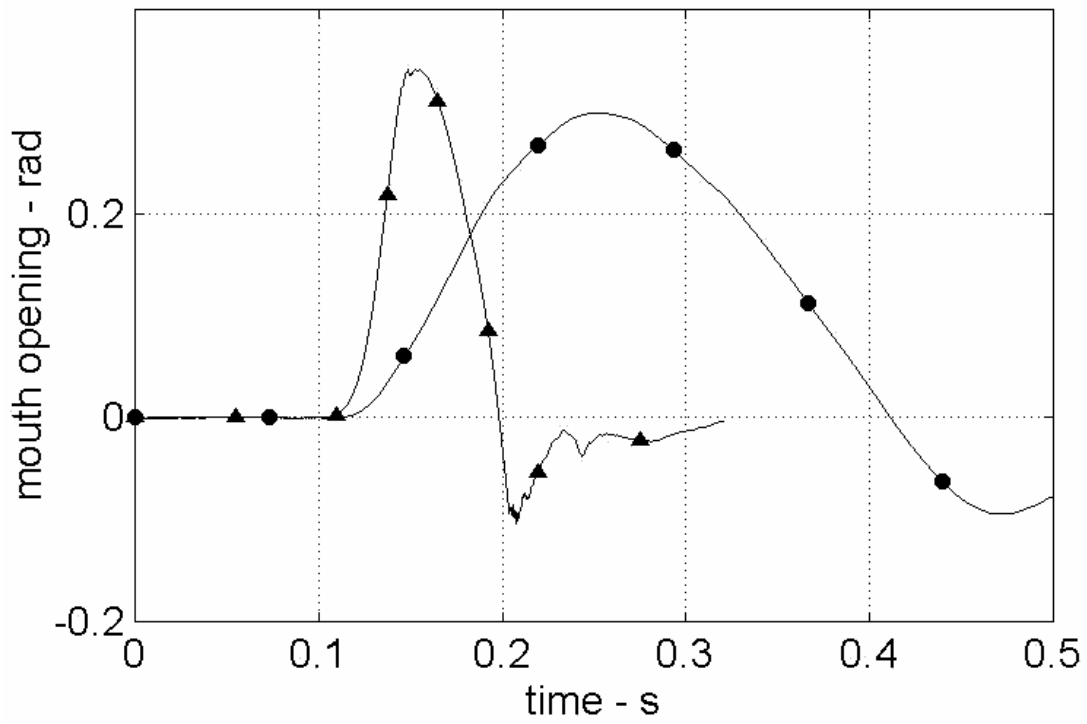


Figure 2. Lyons et al.

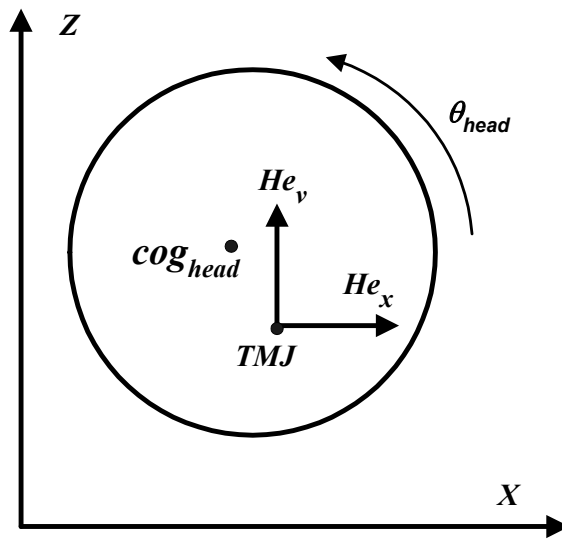


Figure 3. Lyons et al

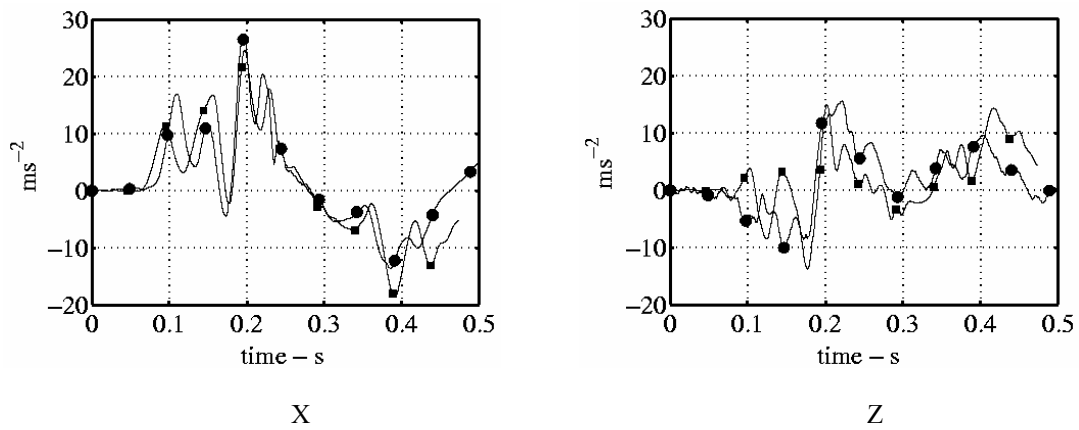


Figure 4. Lyons et al

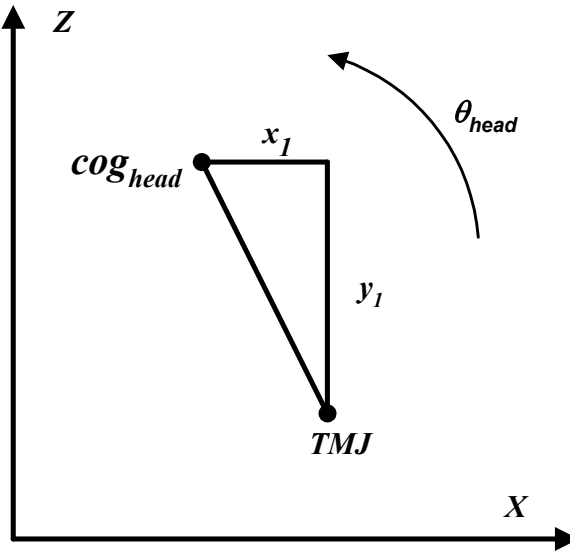


Figure 5. Lyons et al

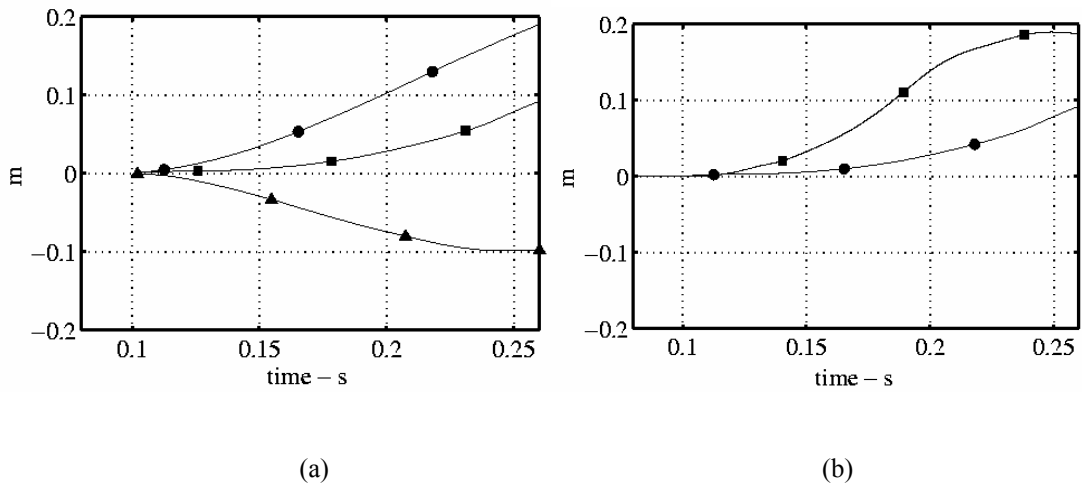


Figure 6. Lyons et al

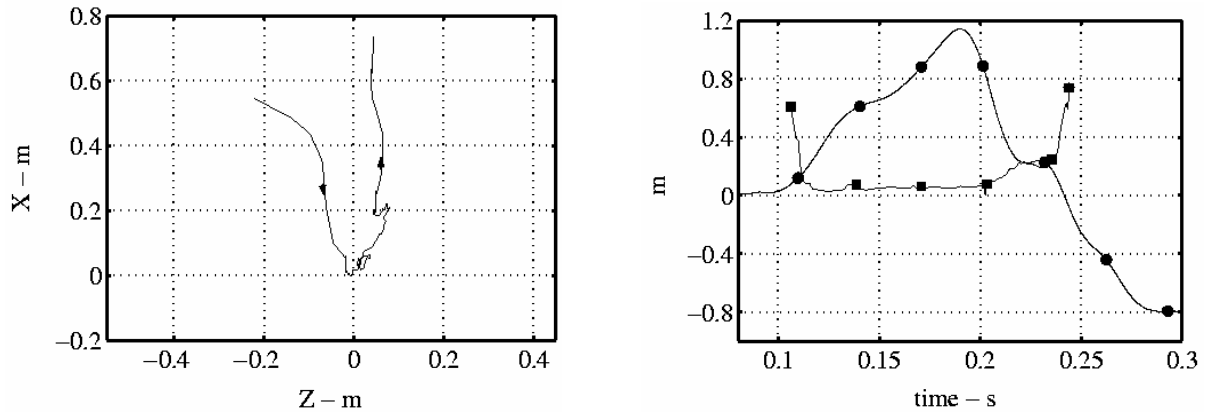


Figure 7. Lyons et al

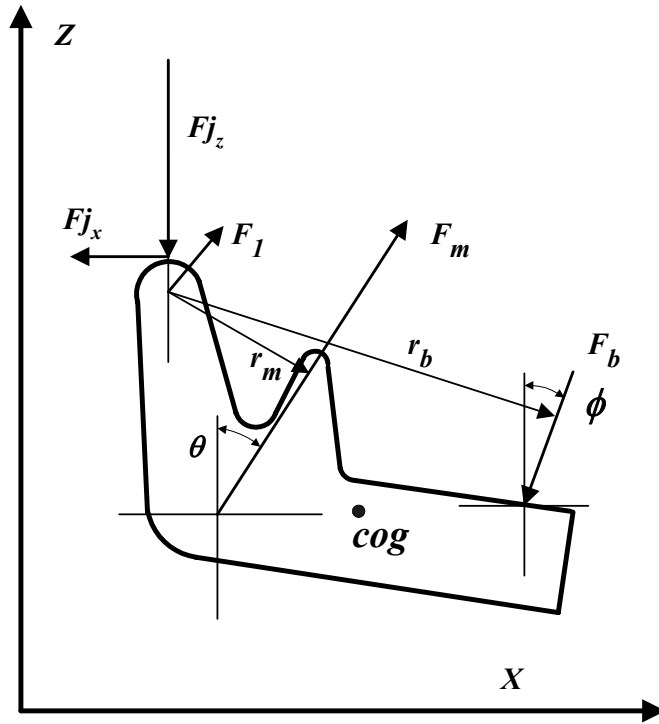


Figure 8. Lyons et al

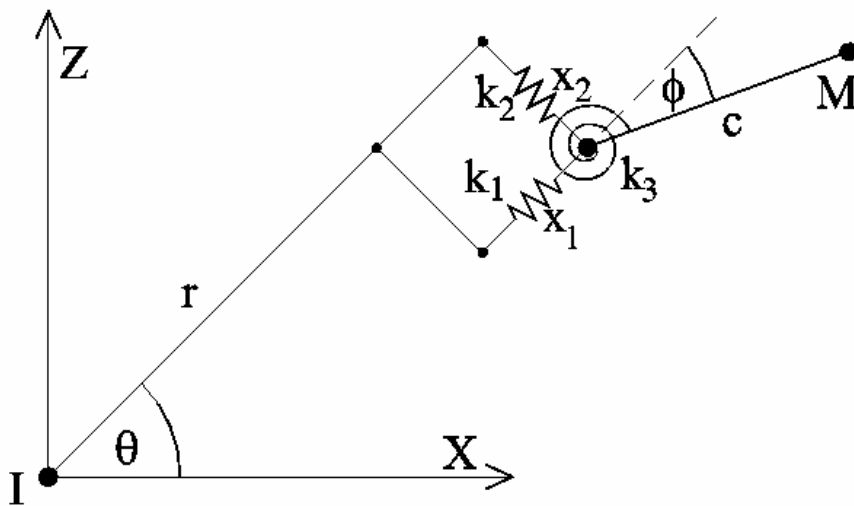


Figure 9. Lyons et al

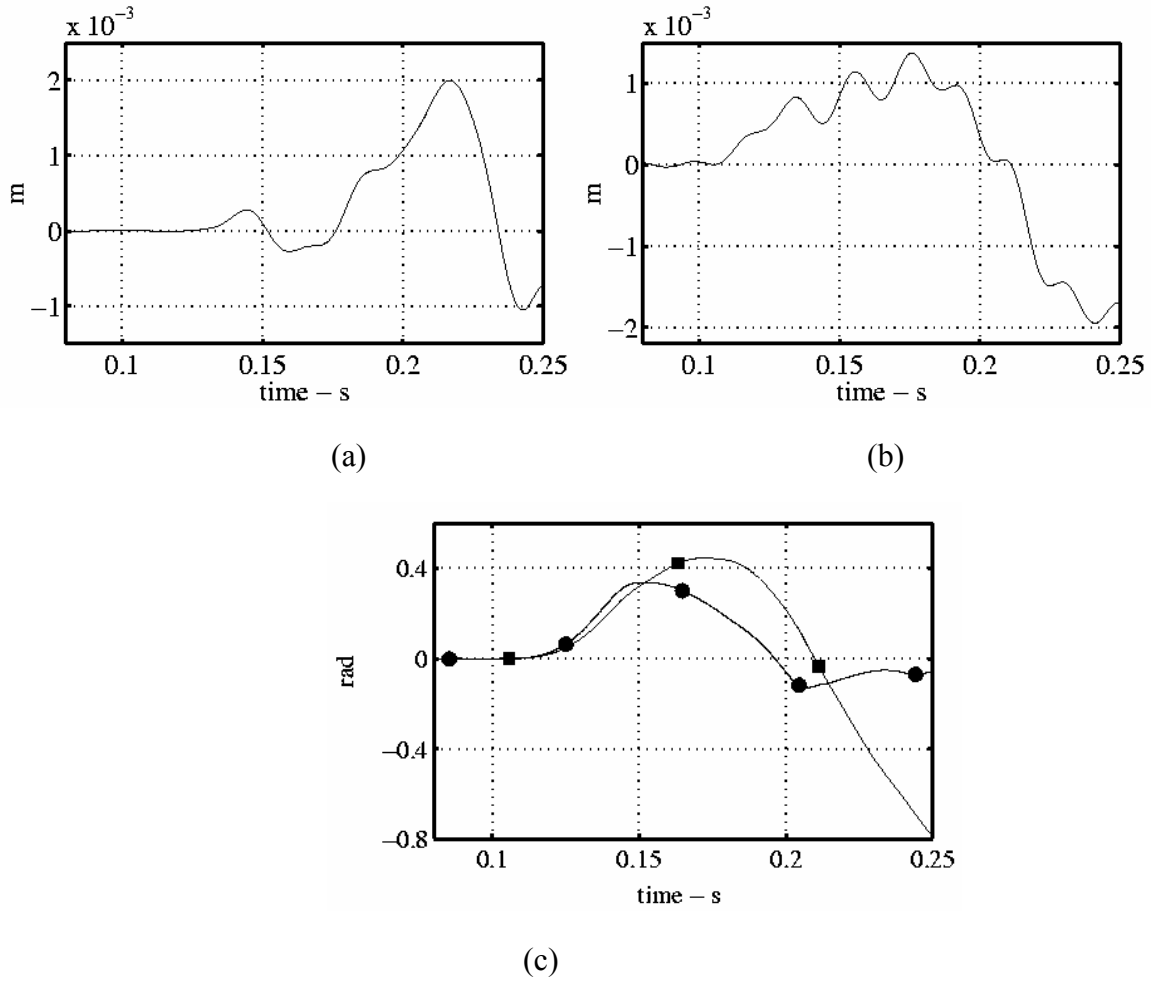


Figure 10. Lyons et al

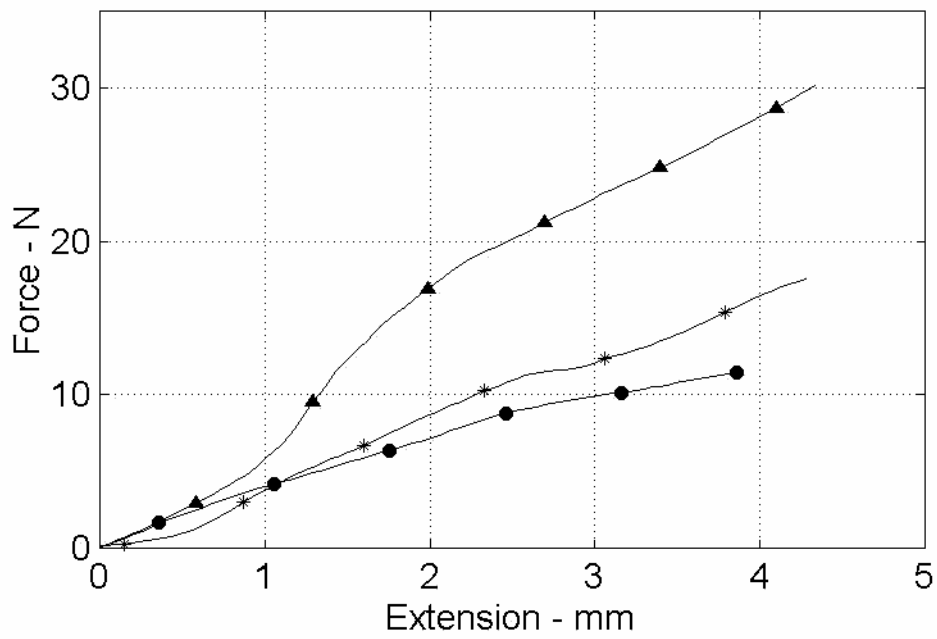


Figure 11 Lyons et al.

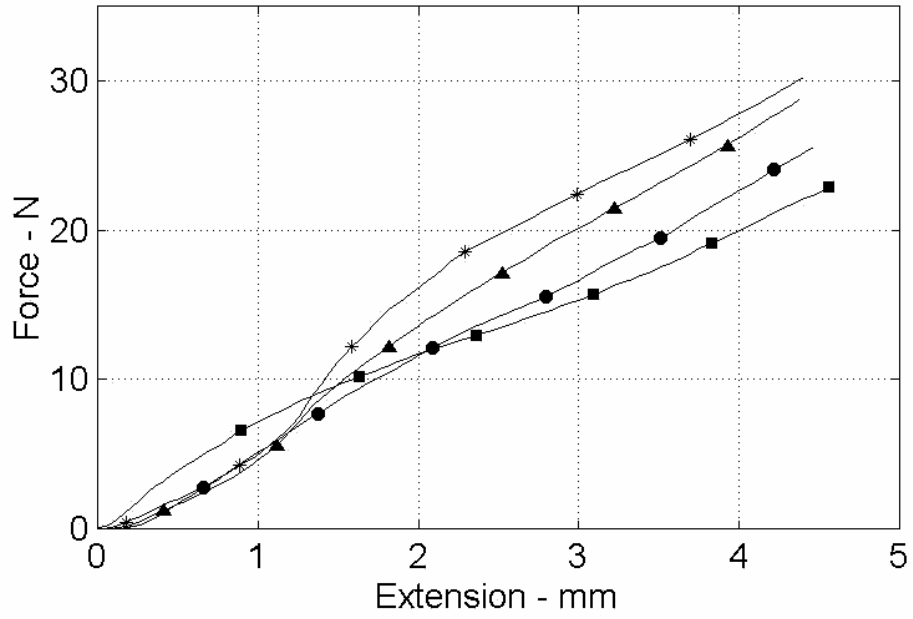


Figure 12 Lyons et al.

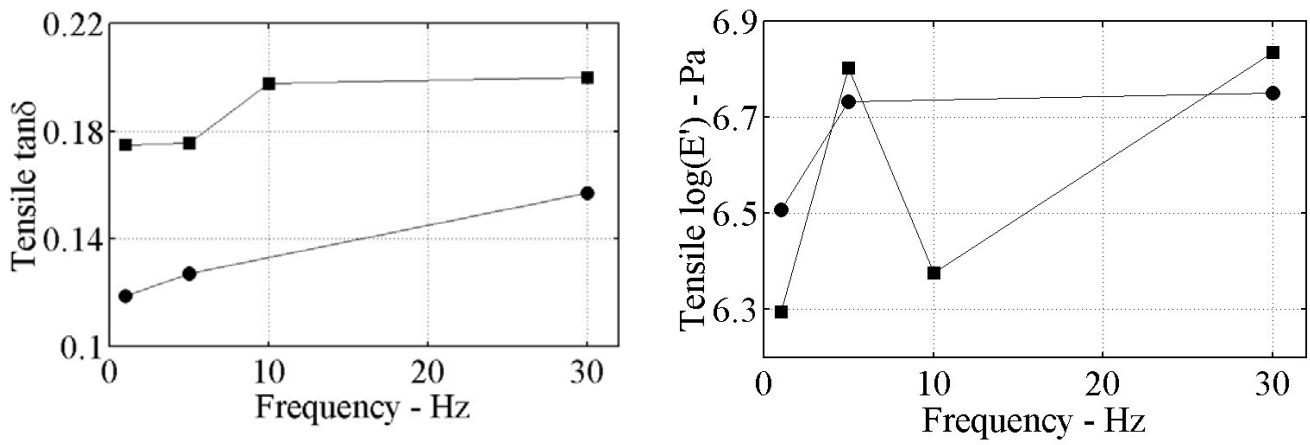


Figure 13 Lyons et al.

List of Figure Captions.

Figure 1. View of the TMJ showing the capsule of the joint and the position of the lateral ligament.

Figure 2. The Dynamics of Mouth Opening During Retroflexion (Mechanistic Model).

(▲) Magnitude of mouth opening, (●) Head rotation (not to scale)

Figure 3. Locations of vertical (He_v) and horizontal (He_h) accelerometers relative to the TMJ and head cog.

Figure 4. TMJ accelerations (skull portion) measured from two locations on the head.

Figure 5. Location of the TMJ relative to the head cog.

Figure 6. (a) X-direction displacements: P_{sled} (●), $P_{\text{head/sled}}$ (▲) and P_{head} (■) and (b) P_{head} (●) and θ_{head} (■) – not to scale.

Figure 7. (a) Locus of head ICR; (b) distance from the TMJ to ICR (■) and $\dot{\theta}_{\text{head}}$ - not to scale – during retroflexion

Figure 8. Free body diagram of the mandible during functional chewing

Figure 9. Kinematic model of the head and TMJ

Figure 10. Simulation results: displacements. (a) x_1 , (b) x_2 , (c) ■ ϕ model, ● ϕ experimental

Figure 11. Force Vs displacement for Cadaveric Specimens- Mouth Closed. (*) Specimen 2, (▲) Specimen 3, (●) Specimen 4.

Figure 12. Force Vs displacement for Cadaveric Specimens- Mouth Open. Specimen 3, (*) 0 degrees, (▲) 5 degrees, (●) 10 degrees, (■) 15 degrees

Figure 13. Variation in $\log(E'')$ and $\tan(\delta)$ of TMJ Ligamentous Tissue with Excitation Frequency (*) sample 1, (●) sample 2.